Intraflagellar transport (IFT) cargo: IFT transports flagellar precursors to the tip and turnover products to the cell body

Hongmin Qin, Dennis R. Diener, Stefan Geimer, Douglas G. Cole, and Joel L. Rosenbaum

Department of Molecular, Cellular, and Developmental Biology, Yale University, New Haven, CT 06520

Intraflagellar transport (IFT) is the bidirectional movement of multisubunit protein particles along axonemal microtubules and is required for assembly and maintenance of eukaryotic flagella and cilia. One posited role of IFT is to transport flagellar precursors to the flagellar tip for assembly. Here, we examine radial spokes, axonemal subunits consisting of 22 polypeptides, as potential cargo for IFT. Radial spokes were found to be partially assembled in the cell body, before being transported to the flagellar tip by anterograde IFT. Fully assembled radial spokes, detached from axonemal microtubules during flagellar breakdown or turnover, are removed from flagella by retrograde IFT. Interactions between IFT particles, motors, radial spokes, and other axonemal proteins were verified by coimmunoprecipitation of these proteins from the soluble fraction of *Chlamydomonas* flagella. These studies indicate that one of the main roles of IFT in flagellar assembly and maintenance is to transport axonemal proteins in and out of the flagellum.

Introduction

The flagellum, in spite of its apparent stability, is a dynamic structure in which the microtubules and appended proteins are constantly turning over (Stephens, 1997; Marshall and Rosenbaum, 2001; Song and Dentler, 2001). The continuous assembly and disassembly of axonemal components at the tip of the flagellum requires the perpetual delivery of precursors to the tip and the removal of discarded flagellar proteins. The 250+ polypeptides that make up the axoneme, therefore, must be transported to the flagellar tip for assembly, not only during flagellar growth, but also for flagellar maintenance in the mature, full-length flagellum.

Many axonemal components are comprised of multiple subunits. For example, outer dynein arms contain 16 different polypeptides (King, 2000) and radial spokes contain 22 (radial spoke protein [RSP]1–22; Piperno et al., 1981; Yang et al., 2001). One mechanism that would simplify targeting, transport, and assembly of flagellar components would be the preassembly of these complexes in the cell body before their delivery into the flagellum. In this way, one targeting sequence could direct an entire complex to the flagellum where it could attach to axonemal microtubules as a completed unit. Such prefabrication would reduce both the number of individual components to be transported and the amount of assembly taking place at the flagellar tip. Early indirect evidence for the presence of stable complexes of flagellar components in the cell body of *Chlamydomonas* was obtained from dikaryon rescue experiments (Luck et al., 1977). Later, more direct evidence for such complexes came from the isolation of an active 22S axonemal dynein from the cytoplasm of deciliated *Paramecium* (Fok et al., 1994) and immunoprecipitation, using an antibody against the dynein β heavy chain, of a dynein complex containing all three dynein heavy chains and both intermediate chains from *Chlamydomonas* cell body extracts (Fowkes and Mitchell, 1998). These results suggest flagellar components can be preassembled in the cell body before entering the flagella.

Flagellar precursors, especially those that are preassembled into large complexes that diffuse slowly, may require a mechanism of transport to the flagellar tip for assembly.

Address correspondence to Joel Rosenbaum, MCDB Dept., Yale University, New Haven, CT 06520. Tel.: (203) 432-3472. Fax: (203) 432-5059. email: joel.rosenbaum@yale.edu

S. Geimer's present address is University of Cologne, Botanical Institute, Gyrhofstrasse 15, 50931 Cologne, Germany.

D.G. Cole's present address is Dept. of Microbiology, Molecular Biology and Biochemistry, University of Idaho, Moscow, ID 83844-3052.

Key words: cilia; intraflagellar; transport; kinesin; radial spoke

Abbreviations used in this paper: IBMX, 3-isobutyl-1-methylxanthine; IFT, intraflagellar transport; M+M, membrane plus matrix; RSP, radial spoke protein.

Intraflagellar transport (IFT) is a likely candidate for this transport. IFT is a microtubule-based motility located between the flagellar membrane and axoneme, in which groups of protein particles are transported from the base to the tip of the flagellum (anterograde) by kinesin II and from the tip to the base (retrograde) by cytoplasmic dynein 1b. The IFT particles are composed of at least 17 polypeptides, which form two complexes, called complex A and B (Piperno and Mead, 1997; Cole et al., 1998; Cole, 2003). This motility, first described in the biflagellate alga *Chlamydomonas*, has been shown to be absolutely essential for the assembly and maintenance of almost all eukaryotic flagella (for review see Rosenbaum and Witman, 2002). Still, many questions remain concerning the role of IFT in ciliary assembly, maintenance, and function.

In the current model of flagellar assembly, IFT particles accumulate around the base of the flagellum at the transitional fibers of the basal bodies (Deane et al., 2001). It is probably in this area that flagellar precursors are loaded onto the IFT particles before being transported to the flagellar tip. Indeed, flagellar precursors are concentrated around the basal bodies in a pattern very similar to that of the IFT particles (Johnson and Rosenbaum, 1992; Piperno et al., 1996). IFT is required to move these precursors to the flagellar tip during flagellar assembly. In the absence of IFT, flagella cannot assemble, and even existing flagella gradually shorten because IFT is required to bring replacement precursors to the flagellar tip to compensate for subunits lost by the continuous turnover at the tip of the axoneme (Marshall and Rosenbaum, 2001).

This study provides the first evidence that IFT serves as a two-way transport system, to bring precursors to the tip for assembly and to return the products of axonemal turnover to the cell body. We have used the radial spoke, one of the principal axonemal components, as a marker for the cargoes of anterograde and retrograde IFT. In the cell body, radial spokes are partially preassembled into 12S complexes, which are moved to the flagellar tip assembly site by anterograde IFT. Once attached to the axoneme the intact (20S) radial spoke is formed. These 20S complexes are released from the axoneme by turnover and are returned to the cell body by retrograde IFT. In addition, we have used antibodies to polypeptides in IFT complex B to show, by immunoprecipitation, that the motors, IFT particles, RSPs, and other axonemal proteins are associated with one another. Immunocytochemistry shows that these components are concentrated in the anterior of the cell surrounding the basal bodies. These data provide the most cogent arguments to date that IFT directly moves flagellar precursors into the flagella and returns spent flagellar components to the cell body.

Results

During flagellar growth, thousands of copies of flagellar precursors must be transported to the flagellar tip for assembly. Transport and assembly of flagellar subunits continue throughout the life of the organelle due to the constant turnover of axonemal components at the flagellar tip. Continuous turnover produces disassembled proteins that must be removed from the flagella. The following experiments were performed to address several questions presented by flagellar assembly and turnover: To what extent are flagellar precursors, in this case the radial spokes, assembled in the cell body before transport into the flagellum? Is IFT directly involved in the transport of these flagellar precursors? What is the fate of disassembled axonemal components–is IFT involved in returning the products of turnover at the flagellar tip to the cell body?

Radial spoke complexes in the cell body and soluble flagellar fraction

Cell body extracts were analyzed on sucrose density gradients to assess the assembly state of radial spokes. Immunoblots of gradient fractions were probed with antibodies to

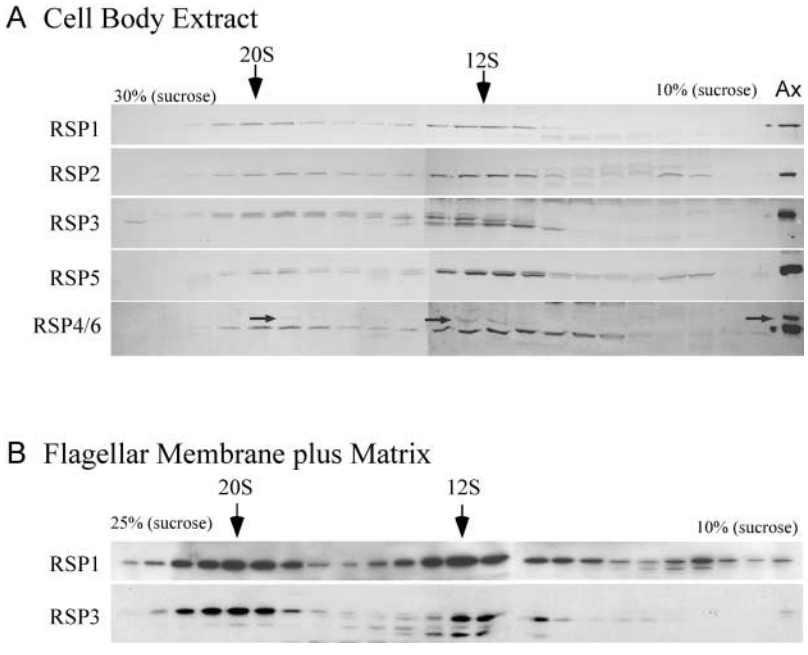

Figure 1. **RSP1–6 from the cell body cosediment on gradients.** (A) Fractions of a sucrose density gradient containing cell body extract were analyzed on immunoblots probed for RSPs as indicated. Note the 12S and 20S peaks of all RSPs examined. RSP3 migrates as a doublet due to phosphorylation; the 20S peak contains the upper phosphorylated band, characteristic of axonemal RSP3, whereas the 12S peak contains both forms. The RSP6 polyclonal antibody cross-reacts with RSP4 (arrows; these two RSPs are 48% identical [Curry et al., 1992]). RSP4 is only faintly visible in the 20S fraction. Ax, axoneme. (B) Gradient analysis of flagellar M+M was performed as in A. Both the 12S and 20S complexes are present in the M+M.

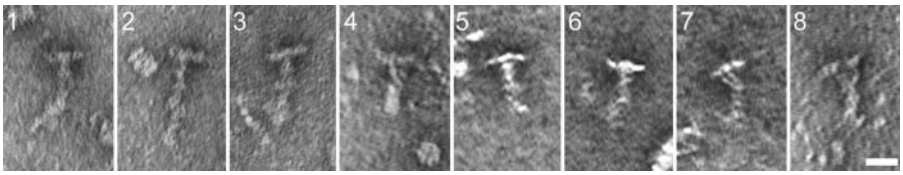

Figure 2. **Negative-stained radial spokes from the 20S membrane plus matrix resemble mature spokes from the axoneme.** Radial spokes from the 20S M+M were generally "T" shaped (panels 1–3), as are mature spokes (Yang et al., 2001); however, in some cases the stalk appeared to be coiled into a helix (panel 4). Occasionally the head formed three or four globular domains tethered to the stalk by thin filaments (panels 5–8). Bar, 20 nm.

three radial spoke head proteins: RSP1, -4, and -6; and three proteins of the radial spoke stalk: RSP3, which attaches the stalk to the axoneme (Huang et al., 1981; Diener et al., 1993), and RSP2 and -5, which may attach the head to the stalk (Huang et al., 1981; Piperno et al., 1981). These six RSPs cosedimented with major peaks at 12S and 20S (Fig. 1 A), suggesting they are assembled into complexes that include the base of the stalk and the head of the spoke. A fraction of some of the RSPs (e.g., RSP2 and -5) were also present in smaller forms, which could represent monomers or small oligomers that had not assembled or that had detached from the larger complexes during preparation. Similar sedimentation analysis of the soluble membrane plus matrix (M+M) fraction isolated from flagella showed that the same 12S and 20S radial spoke complexes were present in this flagellar fraction (Fig. 1 B).

The 20S complex isolated from either the cell body or M+M sediments at the same rate as the intact radial spoke complex extracted from flagellar axonemes with potassium iodide (Yang et al., 2001) and so may be the intact spoke. This complex was examined by EM for comparison to mature spokes (Yang et al., 2001). Because of the low abundance of the complex in the cell body extract, the 20S complex from the M+M was used. In general, negative-stained views of the M+M 20S radial spokes (Fig. 2) were similar to the mature T-shaped spokes extracted from the axoneme (Yang et al., 2001), further suggesting that the 20S complex in the M+M is the complete radial spoke. Some further details of the structure of the spoke from M+M fraction should be noted (Fig. 2). Occasionally, the stalk appeared shorter and thicker than the typical stalk, with a helical substructure. In addition, in some cases the spoke head appeared to be formed of three or four globular domains, which sometimes separated from each other but remained attached to the stalk by thin stems. These differences may have resulted from varying degrees of protein unwinding that occurred during sample preparation, yet they provide new information on the substructure of the radial spoke.

The 12S radial spoke complex is a flagellar precursor carried into the flagellum by IFT

The presence of a subassembly of the radial spoke along with the mature radial spoke in the cell body and M+M raises the question as to their respective functions. The 12S and 20S complexes could represent stages of preassembly of radial spokes in the cell body that are transported through the soluble compartment of the flagellum in transit to the flagellar tip. To test this hypothesis the soluble M+M from growing (regenerating) flagella was isolated and analyzed on gradients. Components in route for flagellar assembly would be expected to be enhanced in the soluble fraction of such flagella. Fig. 3 A shows a gradient of the M+M of half-length, regenerating flagella probed for RSP1. As would be expected for a protein entering the flagellum for assembly, the 12S radial spoke complex was more abundant relative to the 20S complex in regenerating flagella (Fig. 3 A) than in nonregenerating, full-length flagella (Fig. 1 B). This result suggests that the 12S complex, but not the 20S, enters the flagellum to be assembled onto the growing axoneme.

A second observation also suggests that the 12S complex is in route to the flagellar tip for assembly, and also that IFT is the mechanism that transports it there. If IFT carries the

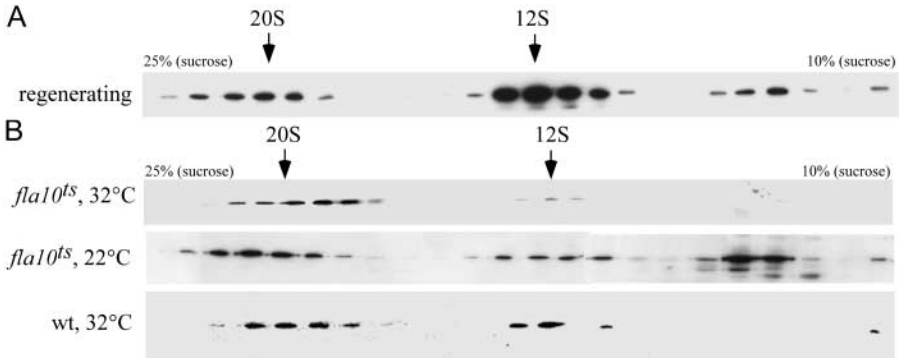

Figure 3. **Radial spoke proteins enter the flagellum as a 12S complex.** (A) M+M fraction from regenerating wild-type cells were separated on 10–25% sucrose density gradients, fractions were separated on 8% gels and blots were probed for RSP1. During flagellar assembly the 12S complex predominates over the 20S complex. (B) Gradient analysis of the M+M of flagella from *fla10*^{ts} cells held at 32°C for 3 h (*fla10*^{ts}, 32°C), shows that the 20S form of radial spokes is more prevalent than the 12S form when IFT is blocked. The shift toward the 20S complex is observed to a lesser degree in *fla10*^{ts} cells at 22°C (*fla10*^{ts}, 22°C), at which temperature other minor effects of the mutation are apparent (Lux and Dutcher, 1991; Kozminski et al., 1995). Wild-type cell body extract is also shown (wt, 32°C) as a control. The blots were probed for RSP1.

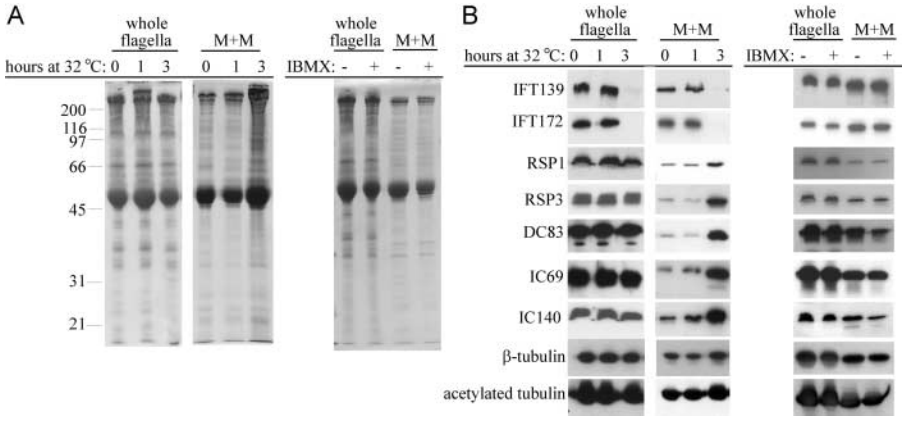

Figure 4. **Disassembled axonemal proteins accumulate in the membrane plus matrix when IFT is blocked.** Flagella were isolated from *fla10*^{ts} cells incubated at 32°C for 0, 1, and 3 h or from wild-type cells treated with 1 mM IBMX for 75 min. Equal amounts of flagellar protein, or the M+M fraction from three times an equivalent amount of flagella, were processed for SDS-PAGE. (A) Coomassie blue–stained 10% gel of whole flagella and M+M. Molecular mass markers are indicated on the left. (B) Corresponding immunoblots probed with antibodies against IFT proteins and a variety of axonemal proteins (Table I). Note in B the disappearance of IFT proteins and the accumulation of axonemal proteins in the M+M of flagella of *fla10*^{ts} cells after 3 h at 32°C, but not in the M+M of flagella of IBMX-treated cells.

12S complex to the tip, blocking anterograde IFT should reduce the amount of 12S precursors in the soluble M+M flagellar fraction. Incubation of the *Chlamydomonas* mutant *fla10*^{ts} at 32°C (restrictive temperature) inactivates the FLA10 subunit of the anterograde IFT motor, FLA10 kinesin II, thereby halting IFT; after 2 h under these conditions IFT can no longer be seen and the flagella start to resorb. Gradient analysis of the M+M from flagella undergoing resorption shows that the concentration of 12S complex decreases (Fig. 3 B) relative to the concentration of 20S. These observations suggest that the 12S radial spoke complex is transported by IFT into the flagella for assembly, but the 20S complex must have a different origin.

The 20S radial spoke complex is a flagellar turnover product removed from the flagellum by IFT

Gradient analysis of the M+M of shortening flagella of *fla10*^{ts} cells showed a change in the relative amounts of 12S and 20S complexes. To examine the absolute change of soluble radial spokes in these flagella, whole flagella and M+M were analyzed by SDS-PAGE and immunoblots. The stained gels (Fig. 4 A) show that for an equal amount of total flagellar protein the amount of soluble protein increases as the flagella shorten after 3 h at 32°C. Immunoblots of these gels (Fig. 4 B) show that IFT particle proteins disappeared by 3 h; however, RSP1 and -3 increased, along with subunits of outer (IC69 and DC83) and inner (IC140) dynein arms, β- and acetylated α-tubulin. The build up of RSPs must be due to the accumulation of the 20S complex (Fig. 3) resulting from the breakdown of the flagellar axoneme in the absence of retrograde IFT, which stops, along with anterograde IFT, in the flagella of *fla10*^{ts} cells incubated at 32°C. This accumulation of axonemal proteins was not seen in flagella induced to shorten by treating cells with 1 mM 3-isobutyl-1-methyxanthine (IBMX; Fig. 4), which induces flagellar resorption (Lefebvre et al., 1978) without affecting IFT (Kozminski et al., 1993). Thus, only in the absence of IFT does flagellar shortening result in the accumulation of the 20S radial spoke complex and other axonemal components in the soluble compartment of resorbing flagella.

IFT probably transports axonemal breakdown products produced by flagellar resorption or, presumably, by turnover, to the cell body. If this is the only source of 20S radial spokes in the cell body, cells without flagella should not contain the 20S complex. Cell body extracts from *bld1*, *bld2*, and *ift88*, *Chlamydomonas* mutants that lack flagella due to mutations in the genes encoding IFT52 (Brazelton et al., 2001), ε-tubulin (Dutcher et al., 2002), and IFT88 (Pazour et al., 2000), respectively, were analyzed on sucrose gradients. These cell body extracts contained the 12S complex, but no detectable 20S form (Fig. 5 A). This result shows that the presence of the 20S complex in the cell body is dependent on the presence of flagella.

The relationship between the 20S radial spoke complex in the cell body and IFT was further explored in two mutants that lack retrograde IFT. Deletion of the gene encoding the heavy chain of the retrograde motor DHC1b results in cells with only flagellar stubs (Pazour et al., 1999; Porter et al., 1999). The cell bodies of this mutant, *dhc1b*, contained no 20S complex (Fig. 5 B). Short flagella (<1 μm) isolated from *dhc1b* cells contain IFT particles and radial spokes but, for unknown reasons, these proteins were largely insoluble in 0.05% NP-40 (unpublished data) and so could not be subjected to gradient analysis. This observation is corroborated by transmission EM observations: IFT particles remain on the axoneme of *stf1* cells (another DHC1b mutant strain) treated with 0.5 or 2% NP-40 (Porter et al., 1999).

Like *dhc1b*, *fla14* cells are defective in retrograde IFT, but the defect is due to a mutation affecting LC8, a light chain of cytoplasmic dynein (Pazour et al., 1998). *fla14* cells are able to form aberrant flagella that fill with IFT particles and slowly resorb. Cell body extracts from these cells revealed no 20S radial spoke complexes even though both 12S and 20S complexes were detectable in the M+M fraction (Fig. 5 B). These data suggest that the 20S radial spoke complex present in the M+M of *fla14* flagella is not recycled into the cell body because retrograde IFT is not functional. Despite the abundance of IFT particles and the lack of retrograde IFT, RSPs did not accumulate in *fla14* flagella (Pazour et al., 1998). Perhaps the absence of LC8, which is a subunit of

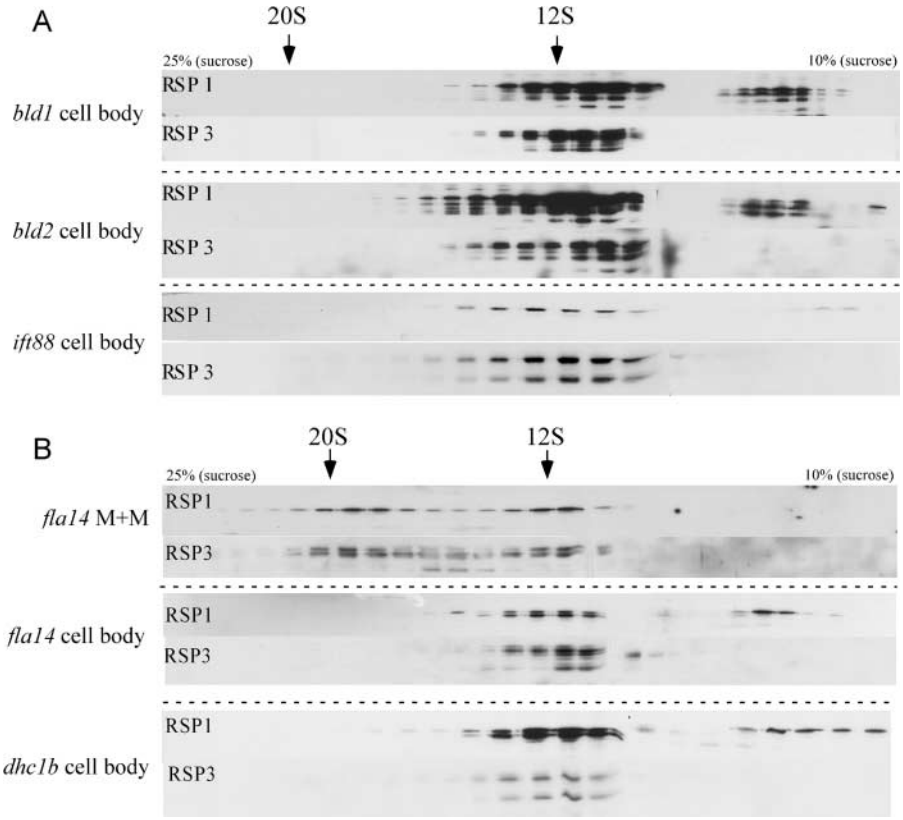

Figure 5. **Retrograde IFT is required for the removal of the 20S radial spoke complex from the flagellum.** (A) Cell body extracts of flagella-less cells were fractionated as in Fig. 3 and the blots were probed for RSP1 and -3. The 20S radial spoke complex present in wild-type cell bodies is absent from mutants without flagella - *bld1*, *bld2*, and *ift88*. (B) Gradient analysis of radial spoke complexes in M+M of *fla14*, which lacks retrograde IFT, shows a normal amount of the 20S complex (*fla14* M+M). No 20S complex is present in the cell body of this mutant (*fla14* cell body) or in *dhc1b* (*dhc1b* cell body), which also lacks retrograde IFT.

multiple flagellar components (King and Patel-King, 1995; Harrison et al., 1998) including radial spokes (Yang et al., 2001), compromises the transport of the 12S and 20S complexes and/or their retention in the flagella.

Coimmunoprecipitation of RSPs with IFT complexes A and B

If IFT directly transports flagellar radial spoke complexes through the flagellum, interactions between IFT complexes A and B, the motors powering their motility, and RSPs should be detectable by immunoprecipitation. In keeping with a previous report (Cole et al., 1998), a monoclonal antibody against complex A protein IFT139, precipitated primarily IFT139 along with the rest of complex A (Fig. 6 B). Similarly, monoclonal antibodies against several complex B proteins (IFT172, IFT81, and IFT57) and a polyclonal antibody against IFT74/72 (α-IFT72$_2$; see Materials and methods), also precipitated predominantly complex B (Fig. 6 B), though a small amount of complex A proteins could be detected in the precipitates (Fig. 6 C). In contrast, polyclonal antibodies against complex B proteins, α-IFT72$_1$ and α-IFT52, precipitated complex B along with approximately stoichiometric amounts of complex A (Fig. 7 B). When these immunoprecipitates were compared with the 16S fraction from M+M, which is enriched in IFT particle proteins, all the IFT proteins of molecular mass >55 kD could be identified (Fig. 7 B); the identity of several of these IFT proteins was confirmed on immunoblots. The IFT proteins of molecular mass <55 kD were presumably present as well but were not detectable by Coomassie blue staining. Precipitation of both complex A and B with either of these complex B antibodies suggests that these complexes interact in vivo.

Immunoprecipitates of α-IFT72$_1$ and α-IFT52, which contained both complex A and B polypeptides, were probed on immunoblots for the presence of the motors

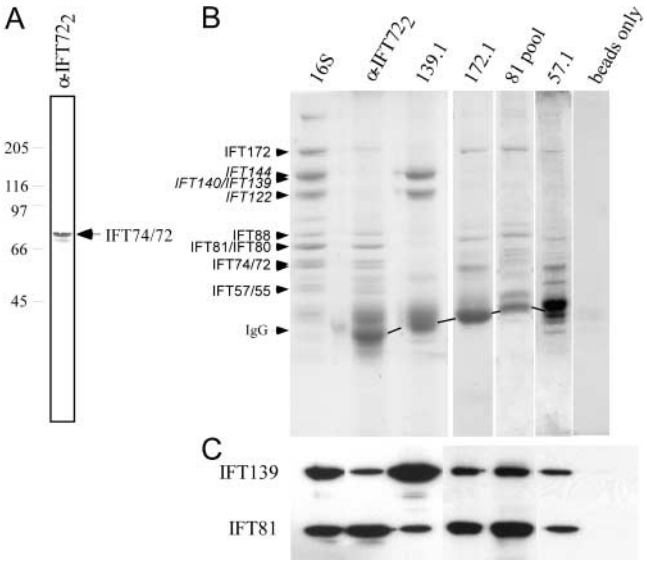

Figure 6. **Intact IFT complex A and B can be immunoprecipitated separately.** (A) Antibody α-IFT72$_2$ recognizes IFT74/72 on an immunoblot of the M+M. (B) Immunoprecipitates with antibodies against IFT polypeptides from M+M were analyzed on Coomassie blue–stained 8% gels. The antibodies used for immunoprecipitation are listed above the gels. The lane labeled 16S shows a sucrose density gradient fraction enriched for IFT polypeptides (Cole et al., 1998). IFT particle complex A (in italics) and B proteins are indicated. (C) Immunoblots of these gels show that IFT81and IFT139 are present in all the immunoprecipitates.

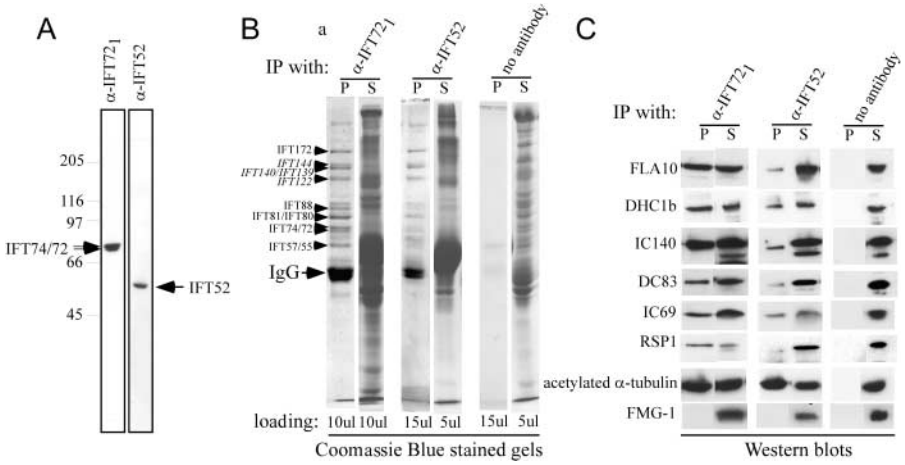

Figure 7. **Complex A and B, IFT motors, and a variety of axonemal proteins coimmunoprecipitate with IFT particles.** (A) Immunoblots of M+M probed with α-IFT72$_1$ and α-IFT52 show these antibodies recognize only the expected proteins. (B) The Coomassie blue–stained gel of immunoprecipitates obtained from M+M using α-IFT72$_1$ and α-IFT52 antibodies show complex A (in italics) and B proteins in the pellet (P), whereas most other proteins remain in the supernatant (S). A control was done without adding antibody (no antibody lanes); similar results were obtained using preimmune serum of α-IFT72$_1$. Pellets were resuspended in sample buffer equal to the supernatant volume. The loading volume is indicated at the bottom of each lane. (C) Corresponding immunoblots probed with antibodies against IFT motors FLA10 and DHC1b, and a variety of flagellar proteins as listed (Table I) show these proteins coprecipitated with IFT proteins. IFT52 is not shown because it is occluded by the IgG heavy chain.

that drive IFT and for axonemal proteins that could represent cargo (Fig. 7 C). Probing blots with antibodies against FLA10 and DHC1b, subunits of the IFT motors, revealed that the anterograde and retrograde IFT motors were both present. In addition to the motors, the immunoprecipitates also contained RSP1, other axonemal proteins, IC69, DC83, IC140, and acetylated α-tubulin indicating that these proteins interact with IFT proteins and are cargo transported by IFT.

It was important to verify that the coimmunoprecipitation of RSPs with IFT proteins was due to specific interactions rather than nonspecific protein trapping. Comparing the proteins in the immunoprecipitates to those remaining in the supernatants demonstrated the specificity of precipitation: many major bands in the supernatant did not appear in the precipitate (Fig. 7 B). Furthermore, FMG-1, the most abundant glycoprotein of the flagellar membrane (Bloodgood et al., 1986), was not immunoprecipitated (Fig. 7 C). As an additional control for nonspecific precipitation, up to 0.5 mg/ml ovalbumin was added to the M+M before immunoprecipitation with α-IFT72$_1$ (Fig. 8 A) and α-IFT52 (unpublished data). Even when assayed by sensitive immunoblotting, there was virtually no detectable ovalbumin in the precipitated pellet. These controls substantiate the specificity of the immunoprecipitation of RSPs and other axonemal proteins with antibodies against IFT particle proteins. In the experiment shown in Fig. 8, ~100% of the IFT proteins were immunoprecipitated. Under these conditions >50% of most of the putative cargoes were coprecipitated (Fig. 8 C). Most of the dynein light chains examined, LC1, LC2, and Tctex1, however, remained in the supernatant. This may be due to their dissociation from the dynein complexes during immunoprecipitation, or they may be transported by a different mechanism.

IFT particle proteins and flagellar protein RSP3 are colocalized at the basal body region

The distribution of IFT52 or FLA10 and a putative cargo, RSP3, in the cell body were compared by immunofluorescence microscopy (Fig. 9), as these proteins had not been examined previously in the same cell. RSP3 was detected in a strain expressing an HA-tagged RSP3 (Diener et al., 1993) using an α-HA antibody. In cells viewed from the side (Fig. 9, see diagram), RSP3 was found surrounding the basal bodies, forming a well-defined "V" shape pointing toward the anterior of the cell. IFT52 had much the same configuration though it had a rounder and more diffuse shape. When viewed from above, RSP3 and IFT52 each formed four spots, two at the periphery of each basal body. Likewise, localization of FLA10 and RSP3 were nearly identical. Thus, the localization of the IFT particles, IFT motors, and RSP cargo in the cell body is consistent with IFT carrying axonemal proteins and suggests the cargo is loaded onto the IFT particles near the basal bodies.

Discussion

Preassembly of radial spokes

Targeting, transport, and assembly of the many proteins required for flagellar assembly could be simplified by a modular construction, in which polypeptides are preassembled in the cell body to form larger subunits of the flagellum, e.g., radial spokes, dynein arms, and central pair projections. The evidence presented here indicates that radial spokes are partially assembled in the cell body to form a 12S complex, which is transported into the flagellum. A radial spoke complex that cosediments at 20S with mature radial spokes extracted from axonemal microtubules is also present in the cell body, but this complex is derived from the turnover of the axoneme, which releases intact radial spokes.

Three observations indicate that the 12S complex is the form of radial spokes used in flagellar assembly. First, the concentration of this complex increases relative to the 20S form in growing flagella in which precursors are needed. Second, the 12S complex, but not the 20S complex, is found in all the flagella-less strains tested, showing it is preassembled in the cell body before flagella are formed. Third, when IFT, which is necessary for flagellar assembly, is inhibited, the 12S radial spoke complex is depleted from the M+M. These observations fit a model in which IFT delivers flagel-

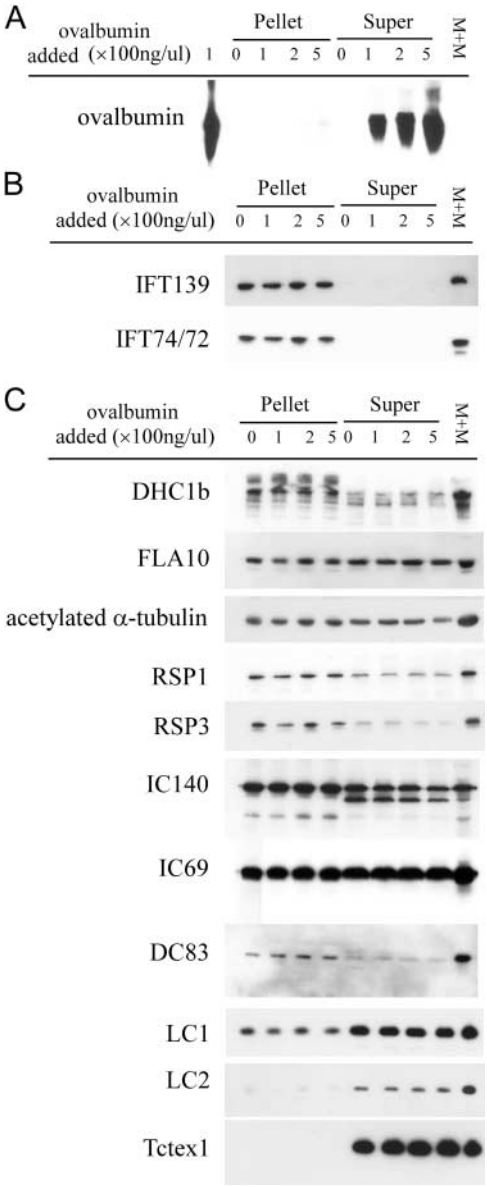

Figure 8. **Immunodepletion of IFT proteins from the membrane plus matrix fraction with α-IFT72$_1$ antibody precipitates a substantial fraction of IFT motors and several axonemal proteins.** Ovalbumin was added to the M+M as a negative control at 100 to 500 ng/μl before immunoprecipitation with α-IFT72$_1$ antibody. Pellets were resuspended in a volume equal to the supernatants and equal volume loadings of pellets (Pellet), supernatants (Super), and M+M were resolved on a 10% gel. Immunoblots show that: (A) ovalbumin did not precipitate; (B) IFT polypeptides were immunodepleted from M+M (exemplified by IFT139 and IFT74/72; the rest of IFT particle proteins were similar; unpublished data); (C) immunoblots with antibodies against IFT motors FLA10 and DHC1b, and a variety flagellar proteins as listed (Table I) show these motor proteins and various flagellar proteins coprecipitated with IFT proteins. In contrast, LC2 and Tctex-1 did not precipitate.

lar precursors to the flagellar tip; in the absence of anterograde IFT, the 12S radial spoke complex and presumably other flagellar precursors are depleted from the flagellum.

The other major radial spoke complex in the cell body and soluble flagellar M+M is a 20S complex that cosediments with mature radial spokes. This form does not appear to be destined for flagellar assembly, but rather, is derived from assembled flagella and is brought back to the cell body by retrograde IFT. This scenario is supported by the observation that the 20S complex decreases relative to the 12S complex in the M+M during flagellar assembly. Furthermore, as flagella resorb due to inhibition of anterograde IFT, the 20S complex increases in the flagellar M+M, indicating it is derived from the breakdown of the axoneme. The 20S complex in the cell body also is derived from the flagella; *Chlamydomonas* mutants that never have flagella do not contain the 20S complex in the cell body although the 12S complex is present. The presence of fully formed flagellar components in the cell body, therefore, is not sufficient to designate these complexes as flagellar precursors destined for assembly.

Assembly of radial spokes occurs in several stages. Although all the RSPs are present, radial spokes are only partially assembled in the cell body. One subassembly made in the cell body is a 12S complex; other subassemblies or monomeric RSPs that go into making the 20S complex could not be identified with the available probes. The mechanism by which the12S complex is converted into the 20S complex in the flagellum, and how this transition is regulated, is still unknown.

Association of IFT particle proteins with axonemal components

When IFT was first described it was hypothesized to be a mechanism for delivering flagellar precursors to the flagellar tip (Kozminski et al., 1993) where assembly occurs (Johnson and Rosenbaum, 1992). Since that time, the IFT particle polypeptides and the motors responsible for their movement have been identified (for reviews see Rosenbaum and Witman, 2002; Sloboda, 2002; Cole, 2003). Mutations affecting IFT proteins or motors have demonstrated that IFT is necessary for both the assembly and maintenance, not only of motile flagella/cilia, but also of immotile, sensory cilia, including the sensory cilia of *Caenorhabditis elegans*. In vertebrates, repercussions of such mutations include diseases such as retinal degeneration, polycystic kidney disease, and the condition known as situs inversus (for review see Rosenbaum and Witman, 2002). Still, little had been learned to confirm or refute the hypothesis that IFT directly transports flagellar precursors.

In perhaps the most direct experiments to test IFT function, inactivation of the FLA10 subunit of the anterograde kinesin II motor blocked the normal addition of inner dynein arms onto existing outer doublet microtubules, presumably because, in the absence of IFT, these components were not transported to the tip (Piperno et al., 1996) where the assembly occurs. In addition, during flagellar regeneration, inner dynein arms were found to sediment at 19S, much faster than sedimentation of a single dynein arm (11S), suggesting the dynein was attached to other molecules during transport in growing flagella (Piperno and Mead, 1997). Still, direct evidence for the association of IFT particles with such axonemal proteins has been lacking.

The immunoprecipitation results presented here provide the first direct evidence that IFT particle proteins bind to axonemal proteins**.** When IFT complexes A and B were im-

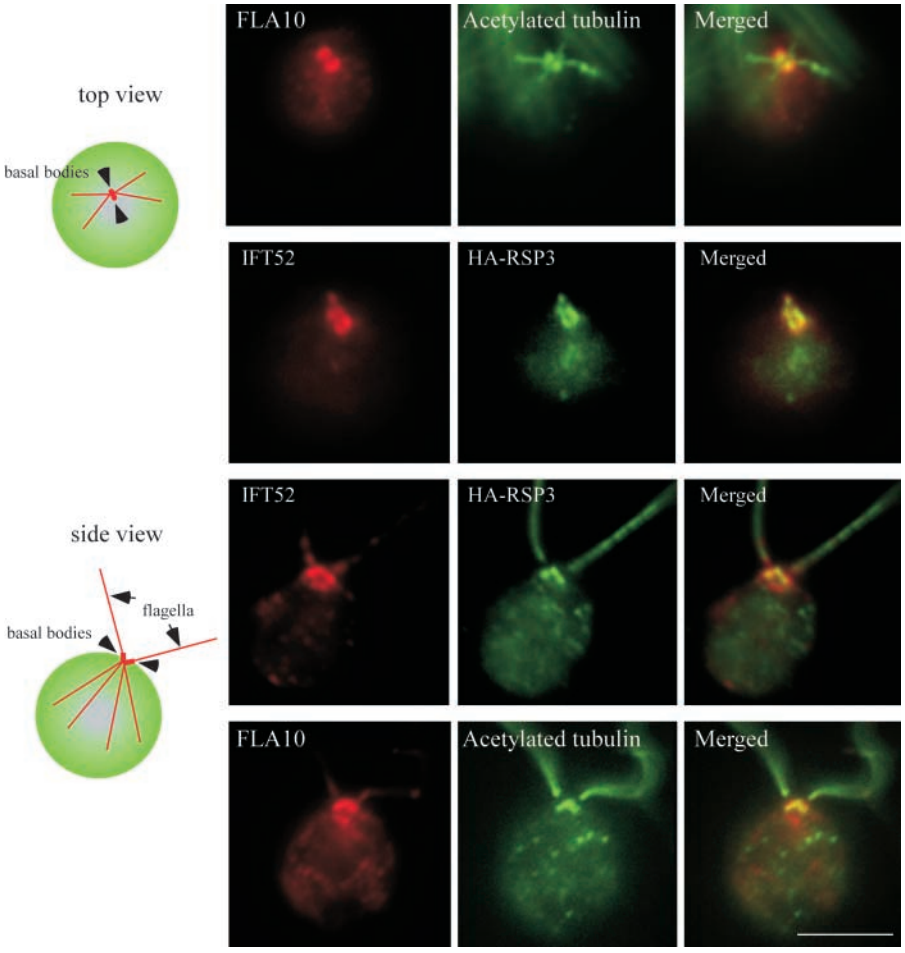

Figure 9. **IFT52 and RSP3 colocalize in the basal body area of the cell.** (Left) Diagrams of the top and side views of a cell showing the position of basal bodies, flagella, and the four microtubule rootlets that emanate from the basal bodies. (Right) Immunofluorescence staining using antibodies as labeled. The first row shows the localization of FLA10 relative to the rootlet microtubules and basal bodies as shown in the diagram. Rows two and three show that the distribution of IFT52 and RSP3 surrounding the basal bodies generally overlap, though IFT52 covers a larger area. The fourth row illustrates the position of FLA10 relative to RSP3. Bar, 5 μm.

munoprecipitated together from the M+M fraction using a polyclonal antibody to a complex B protein, several axonemal proteins were coprecipitated, including RSP1 and -3, subunits of inner and outer dynein arms, and acetylated α-tubulin (Figs. 7 and 8). Conversely, IFT particle proteins could be precipitated with antibodies against IC69, α-tubulin, and acetylated α-tubulin (unpublished data). These results demonstrate that the interactions between IFT proteins and these putative cargo proteins do indeed occur.

In spite of these results, IFT complex A and B sediment on sucrose density gradients without attached motors or cargo, and immunoprecipitation with several IFT antibodies precipitate predominantly only complex A or B proteins. This discrepancy may be due to the avidity of the antibodies. On addition of α-IFT72$_1$ and α-IFT52 antibodies to M+M, a precipitate was often seen, apparently due to the formation of large immunocomplex lattices. The stability and rapid purification of these lattices may explain why these two antibodies precipitated motors and cargos with IFT particles even though the interactions between these molecules may be of too low affinity to be preserved during separation on sucrose density gradients or during precipitation with other antibodies.

Immunofluorescent localization of IFT proteins, FLA10, and axonemal precursors (RSP3) also suggest an interaction between these proteins. Because RSP3 is found throughout the axoneme it was impossible to compare its localization in the flagella to that of IFT52 and FLA10. In the cell body, however, the distribution of these proteins converged in the anterior of the cell in a tight area surrounding the basal bodies. It is apparently in this area that IFT particles and axonemal precursors associate in preparation for transit into the flagellum.

A previous study found that unlike inner arm dynein, outer arm dynein did not require FLA10 to enter the flagellum, and so it might not be a cargo of IFT (Piperno et al., 1996). In the current work, immunoprecipitation of IC69, a component of outer arm dynein, with IFT particles suggests that this dynein can be transported by IFT, though under some circumstances IFT may not be required for its delivery into flagella. IC69 may associate with IFT particles only during its removal from the flagellum as a result of turnover. On the other hand, the original results were obtained by observing *fla10*^{ts} cells after 75 min at 32°C, at which time some attenuated IFT still may be present (Kozminski et al., 1995). Perhaps sufficient IFT was present to transport outer arms to the periphery of the axoneme, but not to transport inner dynein arms to the tip. The relationship between IFT and outer dynein arms is, therefore, not completely resolved.

Association of IFT particle proteins with motors

In addition to binding cargo, IFT particles also would be expected to bind the motors that propel IFT. This report, along with work showing the association of FLA10 and IFT proteins using a microtubule pull down assay (unpublished data),

provides the first direct evidence that IFT proteins are also associated with motors. Immunoprecipitation from M+M with antibodies against IFT74/72 or IFT52 also contained subunits of the anterograde motor, FLA10 kinesin-II, and the retrograde motor, cytoplasmic dynein DHC1B. These motors have also been identified surrounding the basal bodies (Cole et al., 1998; Pazour et al., 1999; Vashishtha et al., 1996) apparently in preparation for taking IFT particles and flagellar components into and out of the flagellum.

The binding of IFT proteins to IFT motors and axonemal precursors suggest that the IFT particles form a link between the IFT motors and cargo as has been described for kinesin (for review see Verhey and Rapoport, 2001) or the dynactin complex, which works in consort with cytoplasmic dynein. In the case of conventional kinesin, for example, c-Jun NH_2-terminal kinase and its associated transmembrane protein ApoRE2 are linked to kinesin by c-Jun NH_2-terminal kinase–interacting proteins, for transport to neurite ends (Verhey et al., 2001). Similarly, the mammalian mLin7/mLin2/mLin10 protein complex is used as a molecular tether between the KIF17 motor and cargo vesicles containing the NR2B subunit of NMDA receptors (Setou et al., 2000). Dynactin is a complex of approximately nine proteins that serves, among other things, to link membranous organelles to the motor cytoplasmic dynein (Holleran et al., 2001; Hoogenraad et al., 2001). The complexity of IFT particles may be in part because they must bridge multiple flagellar cargoes to the anterograde and retrograde motors.

Retrograde IFT

IFT operates continuously in both directions—toward the flagellar tip and back to the cell body. One function of retrograde IFT is to return the IFT particles themselves, and the anterograde IFT motor kinesin II, to the cell body (Iomini et al., 2001; Orozco et al., 1999; Pazour et al., 1998, 1999; Porter et al., 1999; Signor et al., 1999). In the absence of retrograde IFT, e.g., in *dhc1b* and *fla14* mutants, IFT particles accumulate in the flagella blocking assembly and function of the organelles (Pazour et al., 1998, 1999; Porter et al., 1999; Signor et al., 1999). Does retrograde IFT have additional functions?

Several observations suggest that retrograde IFT returns the products of axonemal turnover to the cell body. First is the finding that acetylated α-tubulin immunoprecipitates with IFT particles (Figs. 7 and 8) and so is a potential IFT cargo. Acetylation is a modification of α-tubulin that occurs following tubulin polymerization; soluble tubulin dimers are typically not acetylated (Maruta et al., 1986; Piperno et al., 1987). It seems unlikely, therefore, that acetylated tubulin would be transported from cell body into flagella. Rather, coimmunoprecipitation of acetylated α-tubulin with IFT particles suggests this tubulin was derived from the turnover of axonemal microtubules, which contain acetylated α-tubulin, and is destined to return to the cell body by retrograde IFT.

A second line of evidence for retrograde transport of axonemal breakdown products is that in *fla10^{ts}* cells held at 32°C, radial spokes and other flagellar components accumulate in the flagellar M+M as the flagella slowly begin to shorten (Fig. 4). At this time both anterograde and retrograde IFT no longer function to bring axonemal components in or out of the flagella. As the axonemes shorten the breakdown products accumulate because they cannot be removed from the flagella by IFT. Third, the observation that *fla14* cells, which lack retrograde IFT, contain the 20S radial spoke complex in the M+M, but not in the cell body, also suggests that retrograde IFT carries the products of axonemal breakdown to the cell body. Retrograde IFT, therefore, carries the intact 20S radial spoke complex, as well as other products of flagellar breakdown, out of the flagellum, back to the cell body.

Conclusion

We have used the radial spoke to show that flagellar components are prefabricated in the cell body before their movement into the flagellum. Anterograde IFT is directly involved with the transport of these prefabricated complexes to their assembly site at the flagella tip, and retrograde IFT is responsible for recycling proteins back to the cell body after detachment from the axoneme during flagellar turnover. This is the first clear demonstration that IFT is directly responsible for the transport of a specific flagellar cargo.

Materials and methods

Strains and culture conditions

Chlamydomonas reinhardtii strains used in this work included: wild-type strain cc125, basal body–deficient strain *bld2* (cc478), temperature-sensitive flagellar assembly mutant *fla10* (*fla10–1* allele, cc1919), IFT52 mutant *bld1* (cc477; Brazelton et al., 2001), IFT88 mutant *ift88* (Pazour et al., 2000), cytoplasmic dynein light chain LC8 mutant *fla14* (Pazour et al., 1998), cytoplasmic dynein heavy chain DHC1b mutant *dhc1b* (Pazour et al., 1999), cell wall-less mutant (*cw92*, cc503), paralyzed flagellar mutant *pf14* (cc1032), and a *pf14* strain expressing an HA-tagged RSP3 (Johnson and Rosenbaum, 1992). Strains cc125, cc478, cc1919, cc477, cc503, and cc1032 can be obtained from the *Chlamydomonas* Culture Collection (Duke University, Durham, NC).

Cells were grown on plates or in liquid Tris-acetate-phosphate (Gorman and Levine, 1965) or R/2 (Kindle et al., 1989) medium at 22°C with a light–dark cycle of 14 h:10 h with constant aeration.

Isolation of flagella

Flagellar isolation was essentially as described in Cole et al. (1998). Isolated flagella were resuspended in HMDEK (10 mM Hepes, pH 7.2, 5 mM $MgSO_4$, 1 mM DTT, 0.5 M EDTA, and 25 mM KCl) containing a cocktail of protease inhibitors. *fla14* flagella were isolated when most of the cells had the longest flagella, ~2.5 h after the cells escaped the mother cell wall.

Soluble flagellar proteins, termed the M+M, were extracted from freshly prepared flagella with 0.05% NP-40 in HMDEK. Alternatively, fresh flagella in HMDEK, were flash frozen in liquid nitrogen and thawed to disrupt the flagellar membrane. Axonemal and other insoluble proteins were removed by centrifugation.

Preparation of cytoplasmic extracts

Cells were harvested by centrifugation and the cell pellet was resuspended in an equal volume of HMDEK or lysis buffer: 10 mM Tris, pH 7.4, 5 mM $MgSO_4$, 25 mM KCl, 150 mM NaCl, 0.5 mM EGTA, 1 mM dithiothreitol, and protease inhibitors aprotinin (2 μg/ml), benzamidine (20 μg/ml), pepstatin (1 μg/ml), and trypsin inhibitor (50 μg/ml). Cells (1–5 ml) were disrupted on ice by two 15-s pulses in an Omnimixer (Sorvall) on setting 4. PMSF was added to the homogenate to 1 mM. The homogenate was clarified to remove flagella and cell debris either in a microfuge or at 10,000 rpm in a SW34 rotor (Sorvall) for 10 min and then at 100,000 *g* for 20–60 min in a Ti50 rotor (Beckman Coulter). The clarified extract was typically 20 to 40 mg/ml protein. Cells with cell walls were treated with autolysin for 10 to 60 min before homogenization. Centrifugation was performed at 4°C and the extract was kept on ice.

Sucrose density gradients

M+M or cell body extracts were fractionated through 12-ml 10–25% sucrose density gradients in HMDEK or 10–30% sucrose in lysis buffer (Fig. 1,

A only) in an SW41Ti rotor (Beckman Coulter) for 14 h at 38,000 rpm. Gradients were typically fractionated into 24 to 26 0.5-ml aliquots. Standards used to calculate S-values were BSA (4.4S), aldolase (7.35S), catalase (11.3S), and thyroglobulin (19.4S).

Sequence analysis of IFT74/72

16S IFT particles were purified from *Chlamydomonas* flagella as described in Cole et al. (1998) and separated by PAGE using SDS from EM Science, Inc. Bands corresponding to IFT72 and IFT74 were excised and subjected to microsequence analysis at the University of Massachusetts Medical School Protein Sequencing Facility (Shrewsbury, MA). Five internal peptides were obtained for IFT72: (1) AGQQLQVENRPPP, (2) PAGASIIGAGIT, (3) GEFGSVEDIQR, (4) NLSAGVFEMDEFIK, and (5) VGSQAPVYVIQQEFAALK; and two for IFT74: (1) APTGGAVQQPDRPMTGQR and (2) (Q)VLDKNYFMNEL(R).

To clone *IFT72*, two degenerate primers were designed using the *Chlamydomonas* codon bias to encode part of IFT72 peptides 4 and 5. These primers were used in RT-PCR to amply a partial cDNA of IFT72, which identified several EST clones in Genbank. These EST sequences were used to define the 5′ end of the cDNA sequence and design PCR primers (sequences available on request) to amplify the 3′ end of the IFT72 transcript. The IFT72 cDNA contained a 1,923-nucleotide ORF predicted to encode a 71.4-kD protein with a pI of 9.02 (these sequence data are available from GenBank/EMBL/DDBJ under accession no. AY245434). The five IFT72 peptides were found in the ORF, confirming that it encodes IFT72. IFT72 (from about aa 100 to the COOH-terminal end) is predicted to be a coiled-coil protein.

Several observations suggest IFT72 and IFT74 are derived from the same gene. First, all peptide sequenced from IFT72 and IFT74 were contained in a single ORF, and spanned 96% of the predicted protein. Second, polyclonal antibodies raised against a fragment of IFT72 reacted with both IFT72 and IFT74 (Fig. 7). Third, Southern blot analysis indicated that the *Chlamydomonas* genome contains only one copy of the gene that hybridizes to the IFT72 cDNA (unpublished data). This evidence suggests that IFT72 and IFT74 are isoforms of the same gene product referred to as IFT74/72.

Sequence searches of IFT74/72 revealed the greatest similarity with a putative *C. elegans* protein, C18H9.8 (23% identical, BLASTE E = 7e-30) and a *Ciona intestinalis* protein (these sequence data are available from GenBank/EMBL/DDBJ under accession no. AK115225; 27% identical, BLAST E = 6e-45). The mammalian homologue of IFT74/72 is called CMG-1 (24% identical, BLAST E = 2e-61), a protein that is targeted to an intracellular vesicular compartment and that is differentially expressed during capillary morphogenesis (Bell et al., 2001).

Antibodies and immunoblots

See Table I for a list of antibodies used in this study. The antibodies against RSP2 and -5, though unpublished previously, were generated in parallel

Table I. **Antibodies used in the study**

Protein	Antibody	Type[a]	Reference/Source
IFT particle proteins			
Complex A			
IFT139	139.1	M	Cole et al., 1998
Complex B			
IFT 172	172.1	M	Cole et al., 1998
IFT81	81.1–4 (pooled)	M	Cole et al., 1998
IFT57	57.1	M	Cole et al., 1998
FT52	α-IFT52	P	Deane et al., 2001
IFT74/72	α-IFT72$_1$, α-IFT72$_2$	P	This paper
Kinesin II motor			
FLA10 neck	α-FLA10N	P	Cole et al., 1998
FLA10 tail	α-FLA10T	P	Kozminski et al., 1995
Cytoplasmic dynein heavy chain			
DHC1b	α-DHC1b	P	Pazour et al., 1999
Outer arm dynein			
Intermediate chain			
IC69	α-IC69	M	Sigma-Aldrich
Docking complex			
DC83	α-DC83	P	Wakabayashi et al., 2001
Light chain			
LC1	α-LC1	P	Benashski et al., 1999
LC2	α-LC2	P	Patel-King et al., 1997
Inner arm dynein			
Light chain			
Tctex-1	α-Tctex-1	P	Harrison et al., 1998
Intermediate chain			
IC140	α-IC140		Yang and Sale, 1998
RSPs			
RSP1	α-RSP1	P	Williams et al., 1986
RSP3	α-RSP3	P	Williams et al., 1989
Tubulin			
Acetylated α-tubulin		M	Sigma-Aldrich
β-Tubulin		P	Silflow and Rosenbaum, 1981
Flagellar membrane glycoprotein			
FMG-1	α-FMG-1	M	Bloodgood et al., 1986
Hemagglutinin epitope	12CA5	M	Field et al., 1988
Ovalbumin	α-Ovalbumin	M	Sigma-Aldrich

[a]M, monoclonal; P, polyclonal.

with RSP1, -3, and -6, which have been described previously (Williams et al., 1986, 1989).

Polyclonal α-IFT72$_1$ and α-IFT72$_2$ antisera were raised against the IFT74/72 COOH-terminal domain as follows: The fragment encoding residues 207–641 of IFT74/72 was cloned into the pQE-30 expression vector (QIAGEN) to produce a His6–IFT74/72 fusion protein. The fusion protein was injected subcutaneously into two rabbits by the Yale Biotechnology Services (New Haven, CT) to produce antisera named α-IFT72$_1$ and α-IFT72$_2$. Antibodies were affinity purified from His6–IFT74/72 fusion protein bound to nitrocellulose.

Immunoprecipitation

Flagellar M+M (protein concentration at 5–10 mg/ml) was clarified for 10 min at 100,000 *g* and was then incubated with antibodies on ice for 1–2 h. Immune complexes were recovered by incubation for 2–8 h at 4°C with protein A–Sepharose beads (Amersham Biosciences). After washing three times with 1 ml HMDEK plus 0.05% NP-40 and once with HMDEK plus 300 mM NaCl for 15 min each at RT, proteins were eluted from the beads in SDS-PAGE loading buffer and analyzed by SDS-PAGE followed by immunoblotting.

Immunofluorescence microscopy

Immunofluorescence staining was performed as described previously (Cole et al., 1998). Preparations were photographed on a Nikon Diaphot inverted fluorescence microscope with an Image Point CCD camera (Photometrics) and the Metamorph software package.

Negative staining and EM

Samples taken from gradient fractions were used directly, or were first dialyzed against HMDEK to remove the sucrose, and were applied to 300-mesh copper holey grids covered previously with a thin layer of carbon and activated by glow discharge. Negative staining with uranyl acetate was performed using a modification of the double carbon layer technique (Stoffler-Meilicke and Stoffler, 1988) as described by Koonce and Samso (1996). Samples were examined in a Philips EM 201 operated at 80 kV. Most images were recorded at a magnification of 45,000 using Kodak 4489 EM film.

We thank Drs. P. Yang and W. Sale for providing us with the method for isolating intact radial spokes from axonemes before the publication of their work. We also thank Hue Tran for excellent technical support, Drs. G. Pazour, G. Witman, R. Kamiya, R.A. Bloodgood, S. King, and W. Sale for generously sharing antibodies, W.F. Marshall (Yale University), L. Pedersen (Yale University), and M.M. Barr (University of Wisconsin-Madison, Madison, WI) for helpful discussions and careful reading of the manuscript.

This work was supported by National Institutes of Health grant GM14642 to J.L. Rosenbaum, a Polycystic Kidney Disease Foundation fellowship to H. Qin, and a Deutsche Forschungsgemeinschaft (GE 1110/2-1) fellowship to S. Geimer.

Submitted: 25 August 2003
Accepted: 24 November 2003

References

Bell, S.E., A. Mavila, R. Salazar, K.J. Bayless, S. Kanagala, S.A. Maxwell, and G.E. Davis. 2001. Differential gene expression during capillary morphogenesis in 3D collagen matrices: regulated expression of genes involved in basement membrane matrix assembly, cell cycle progression, cellular differentiation and G-protein signaling. *J. Cell Sci.* 114:2755–2773.

Benashski, S.E., R.S. Patel-King, and S.M. King. 1999. Light chain 1 from the *Chlamydomonas* outer dynein arm is a leucine-rich repeat protein associated with the motor domain of the heavy chain. *Biochemistry.* 38:7253–7264.

Bloodgood, R.A., M.P. Woodward, and N.L. Salomonsky. 1986. Redistribution and shedding of flagellar membrane glycoproteins visualized using an anti-carbohydrate monoclonal antibody and concanavalin A. *J. Cell Biol.* 102: 1797–1812.

Brazelton, W., C. Amundsen, C. Silflow, and P. Lefebvre. 2001. The *bld1* mutation identifies the *Chlamydomonas osm-6* homolog as a gene required for flagellar assembly. *Curr. Biol.* 11:1591–1594.

Cole, D.G. 2003. The intraflagellar transport machinery of *Chlamydomonas reinhardtii*. *Traffic.* 4:435–442.

Cole, D.G., D.R. Diener, A.L. Himelblau, P.L. Beech, J.C. Fuster, and J.L. Rosenbaum. 1998. *Chlamydomonas* kinesin-II–dependent intraflagellar transport (IFT): IFT particles contain proteins required for ciliary assembly in *Caenorhabditis elegans* sensory neurons. *J. Cell Biol.* 141:993–1008.

Curry, A.M., B.D. Williams, and J.L. Rosenbaum. 1992. Sequence analysis reveals homology between two proteins of the flagellar radial spoke. *Mol. Cell. Biol.* 12:3967–3977.

Deane, J.A., D.G. Cole, E.S. Seeley, D.R. Diener, and J.L. Rosenbaum. 2001. Localization of intraflagellar transport protein IFT52 identifies basal body transitional fibers as the docking site for IFT particles. *Curr. Biol.* 11:1586–1590.

Diener, D.R., L.H. Ang, and J.L. Rosenbaum. 1993. Assembly of flagellar radial spoke proteins in *Chlamydomonas*: identification of the axoneme binding domain of radial spoke protein 3. *J. Cell Biol.* 123:183–190.

Dutcher, S.K., N.S. Morrissette, A.M. Preble, C. Rackley, and J. Stanga. 2002. Epsilon-tubulin is an essential component of the centriole. *Mol. Biol. Cell.* 13: 3859–3869.

Field, J., J.-I. Nikawa, D. Broek, B. MacDonald, L. Rodgers, I.A. Wilson, R.A. Lerner, and M. Wigler. 1988. Purification of a RAS-responsive adenylyl cyclase complex from *Saccharomyces cerevisiae* by use of an epitope addition method. *Mol. Cell. Biol.* 8:2159–2165.

Fok, A.K., H. Wang, A. Katayama, M.S. Aihara, and R.D. Allen. 1994. 22S Axonemal dynein is preassembled and functional prior to being transported to and attached on the axonemes. *Cell Motil. Cytoskeleton.* 29:215–224.

Fowkes, M.E., and D.R. Mitchell. 1998. The role of preassembled cytoplasmic complexes in assembly of flagellar dynein subunits. *Mol. Biol. Cell.* 9:2337–2347.

Gorman, D.S., and R.P. Levine. 1965. Cytochrome f and plastocyanin: their sequence in photosynthetic electron transport chain of *Chlamydomonas reinhardi*. *Proc. Natl. Acad. Sci. USA.* 54:1665–1669.

Harrison, A., P. Olds-Clarke, and S.M. King. 1998. Identification of the t complex-encoded cytoplasmic dynein light chain Tctex1 in inner arm I1 supports the involvement of flagellar dyneins in meiotic drive. *J. Cell Biol.* 140: 1137–1147.

Holleran, E., L. Ligon, T. Mariko, M. Stankewich, J.S. Morrow, and E. Holzbaur. 2001. βIII spectrin binds to the arp1 subunit of dynactin. *J. Biol. Chem.* 276:36598–36605.

Hoogenraad, C., A. Akhmanova, S. Howell, B. Dortland, C. De Zeeuw, R. Willemsen, P. Visser, F. Grosveld, and N. Galjart. 2001. Mammalian Golgi-associated Bicaudal-D2 functions in the dynein-dynactin pathway by interacting with these complexes. *EMBO J.* 20:4041–4054.

Huang, B., G. Piperno, Z. Ramanis, and D.J.L. Luck. 1981. Radial spokes of *Chlamydomonas* flagella: genetic analysis of assembly and function. *J. Cell Biol.* 88:80–88.

Iomini, C., V. Bebaev-Khaimov, M. Sassaroli, and G. Piperno. 2001. Protein particles in *Chlamydomonas* flagella undergo a transport cycle consisting of four phases. *J. Cell Biol.* 153:13–24.

Johnson, K.A., and J.L. Rosenbaum. 1992. Polarity of flagellar assembly in *Chlamydomonas*. *J. Cell Biol.* 119:1605–1611.

Kindle, K.L., R.A. Schnell, E. Fernandez, and P.A. Lefebvre. 1989. Stable nuclear transformation of *Chlamydomonas* using the *Chlamydomonas* gene for nitrate reductase. *J. Cell Biol.* 109:2589–2601.

King, S.M. 2000. The dynein microtubule motor. *Biochim. Biophys. Acta.* 1496: 60–75.

King, S.M., and R.S. Patel-King. 1995. The M(r) = 8,000 and 11,000 outer arm dynein light chains from *Chlamydomonas* flagella have cytoplasmic homologues. *J. Biol. Chem.* 270:11445–11452.

Kozminski, K.G., K.A. Johnson, P. Forscher, and J.L. Rosenbaum. 1993. A motility in the eukaryotic flagellum unrelated to flagellar beating. *Proc. Natl. Acad. Sci. USA.* 90:5519–5523.

Kozminski, K.G., P.L. Beech, and J.L. Rosenbaum. 1995. The *Chlamydomonas* kinesin-like protein FLA10 is involved in motility associated with the flagellar membrane. *J. Cell Biol.* 131:1517–1527.

Koonce, M.P., and M. Samso. 1996. Overexpression of cytoplasmic dynein's globular head causes a collapse of the interphase microtubule network in *Dictyostelium*. *Mol. Biol. Cell.* 7:935–948.

Lefebvre, P.A., S.A. Nordstrom, J.E. Moulder, and J.L. Rosenbaum. 1978. Flagellar elongation and shortening in *Chlamydomonas* IV. Effects of flagellar detachment, regeneration, and resorption on the induction of flagellar protein synthesis. *J. Cell Biol.* 78:8–27.

Luck, D., G. Piperno, Z. Ramanis, and B. Huang. 1977. Flagellar mutants of *Chlamydomonas*: studies of radial spoke-defective strains by dikaryon and re-

vertant analysis. *Proc. Natl. Acad. Sci. USA.* 74:3456–3460.

Lux, F.G., III, and S.K. Dutcher. 1991. Genetic interactions at the FLA10 locus: suppressors and synthetic phenotypes that affect the cell cycle and flagellar function in *Chlamydomonas reinhardtii. Genetics.* 128:549–561.

Marshall, W.F., and J.L. Rosenbaum. 2001. Intraflagellar transport balances continuous turnover of outer doublet microtubules: implications for flagellar length control. *J. Cell Biol.* 155:405–414.

Maruta, H., K. Greer, and J.L. Rosenbaum. 1986. The acetylation of alpha-tubulin and its relationship to the assembly and disassembly of microtubules. *J. Cell Biol.* 103:571–579.

Orozco, J.T., K.P. Wedaman, D. Signor, H. Brown, L. Rose, and J.M. Scholey. 1999. Movement of motor and cargo along cilia. *Nature.* 398:674.

Patel-King, R.S., S.E. Benashski, A. Harrison, and S.M. King. 1997. A *Chlamydomonas* homologue of the putative murine t complex distorter Tctex-2 is an outer arm dynein light chain. *J. Cell Biol.* 137:1081–1090.

Pazour, G.J., B.L. Dickert, Y. Vucica, E.S. Seeley, J.L. Rosenbaum, G.B. Witman, and D.G. Cole. 2000. *Chlamydomonas* IFT88 and its mouse homologue, polycystic kidney disease gene tg737, are required for assembly of cilia and flagella. *J. Cell Biol.* 151:709–718.

Pazour, G.J., B.L. Dickert, and G.B. Witman. 1999. The DHC1b (DHC2) isoform of cytoplasmic dynein is required for flagellar assembly. *J. Cell Biol.* 144:473–481.

Pazour, G.J., C.G. Wilkerson, and G.B. Witman. 1998. A dynein light chain is essential for retrograde particle movement in intraflagellar transport (IFT). *J. Cell Biol.* 141:979–992.

Piperno, G., B. Huang, Z. Ramanis, and D.J.L. Luck. 1981. Radial spokes of *Chlamydomonas* flagella: polypeptide composition and phosphorylation of stalk components. *J. Cell Biol.* 88:73–79.

Piperno, G., M. LeDizet, and X.-J. Chang. 1987. Microtubules containing acetylated α-tubulin in mammalian cells in culture. *J. Cell Biol.* 104:289–302.

Piperno, G., and K. Mead. 1997. Transport of a novel complex in the cytoplasmic matrix of *Chlamydomonas* flagella. *Proc. Natl. Acad. Sci. USA.* 94:4457–4462.

Piperno, G., K. Mead, and S. Henderson. 1996. Inner dynein arms but not outer dynein arms require the activity of kinesin homologue protein KHP1FLA10 to reach the distal part of flagella in *Chlamydomonas. J. Cell Biol.* 133:371–379.

Porter, M.E., R. Bower, J.A. Knott, P. Byrd, and W. Dentler. 1999. Cytoplasmic dynein heavy chain 1b is required for flagellar assembly in *Chlamydomonas. Mol. Biol. Cell.* 10:693–712.

Rosenbaum, J.L., and G.B. Witman. 2002. Intraflagellar transport. *Nat. Rev. Mol. Cell Biol.* 3:813–825.

Setou, M., T. Nakagawa, D. Seog, and N. Hirokawa. 2000. Kinesin superfamily motor protein KIF17 and mLin-10 in NMDA receptor-containing vesicle transport. *Science.* 288:1796–1802.

Signor, D., K.P. Wedaman, J.T. Orozco, N.D. Dwyer, C.I. Bargmann, L.S. Rose, and J.M. Scholey. 1999. Role of a class DHC1b dynein in retrograde transport of IFT motors and IFT raft particles along cilia, but not dendrites, in chemosensory neurons of living *Caenorhabditis elegans. J. Cell Biol.* 147: 519–530.

Silflow, C.D., and J.L. Rosenbaum. 1981. Multiple α- and β-tubulin genes in *Chlamydomonas* and regulation of tubulin mRNA levels after deflagellation. *Cell.* 24:81–88.

Sloboda, R. 2002. A healthy understanding of intraflagellar transport. *Cell Motil. Cytoskeleton.* 52:1–8.

Song, L., and W.L. Dentler. 2001. Flagellar protein dynamics in *Chlamydomonas. J. Biol. Chem.* 276:29754–29763.

Stephens, R.E. 1997. Synthesis and turnover of embryonic sea urchin ciliary proteins during selective inhibition of tubulin synthesis and assembly. *Mol. Biol. Cell.* 8:2187–2198.

Stoffler-Meilicke, M., and G. Stoffler. 1988. Localization of ribosomal proteins on the surface of ribosomal subunits from *Escherichia coli* using immunoelectron microscopy. *Methods Enzymol.* 164:503–520.

Vashishtha, M., Z. Walther, and J.L. Hall. 1996. The kinesin-homologous protein encoded by the *Chlamydomonas* FLA10 gene is associated with basal bodies and centrioles. *J. Cell Sci.* 109:541–549.

Verhey, K., D. Meyer, R. Deehan, J. Blenis, B. Schnapp, T. Rapoport, and B. Margolis. 2001. Cargo of kinesin identified as JIP scaffolding proteins and associated signaling molecules. *J. Cell Biol.* 152:959–970.

Verhey, K., and T. Rapoport. 2001. Kinesin carries the signal. *Trends Biochem. Sci.* 26:545–550.

Wakabayashi, K., S. Takada, G.B. Witman, and R. Kamiya. 2001. Transport and arrangement of the outer-dynein-arm docking complex in the flagella of *Chlamydomonas* mutants that lack outer dynein arms. *Cell Motil. Cytoskeleton.* 48:277–286.

Williams, B.D., D.R. Mitchell, and J.L. Rosenbaum. 1986. Molecular cloning and expression of flagellar radial spoke and dynein genes of *Chlamydomonas. J. Cell Biol.* 103:1–11.

Williams, B.D., M.A. Velleca, A.M. Curry, and J.L. Rosenbaum. 1989. Molecular cloning and sequence analysis of the *Chlamydomonas* gene coding for radial spoke protein 3: flagellar mutation *pf-14* is an ochre allele. *J. Cell Biol.* 109: 235–245.

Yang, P., D.R. Diener, J.L. Rosenbaum, and W.S. Sale. 2001. Localization of calmodulin and dynein light chain LC8 in flagellar radial spokes. *J. Cell Biol.* 153:1315–1326.

Yang, P., and W. Sale. 1998. The Mr 140,000 intermediate chain of *Chlamydomonas* flagellar inner arm dynein is a WD-repeat protein implicated in dynein arm anchoring. *Mol. Biol. Cell.* 9:3335–3349.

Hongmin Qin, Dennis R. Diener, Stefan Geimer, Douglas G. Cole, and Joel L. Rosenbaum

Vol. 164, No. 2, January 19, 2004. Pages 255–266.

Due to a printer error, Figure 9 was mislabeled. The bottom-center panel should have read "HA-RSP3" instead of "Acetylated tubulin." The corrected figure appears below.